

Evidence for Nonreciprocal Organization of the Mouse Auditory Thalamocortical-Corticothalamic Projection Systems

DANIEL A. LLANO^{1*} AND S. MURRAY SHERMAN²

¹Department of Neurology, University of Chicago, Chicago, Illinois 60637

²Department of Neurobiology, University of Chicago, Chicago, Illinois 60637

ABSTRACT

We tested the hypothesis that information is routed from one area of the auditory cortex (AC) to another via the dorsal division of the medial geniculate body (MGBd) by analyzing the degree of reciprocal connectivity between the auditory thalamus and cortex. Biotinylated dextran amine injected into the primary AC (AI) or anterior auditory field (AAF) of mice produced large, “driver-type” terminals primarily in the MGBd, with essentially no such terminals in the ventral MGB (MGBv). In contrast, small, “modulator-type” terminals were found primarily in the MGBv, and this coincided with areas of retrogradely labeled thalamocortical cell bodies. After MGBv injections, anterograde label was observed in layers 4 and 6 of the AI and AAF, which coincided with retrogradely labeled layer 6 cell bodies. After MGBd injections, thalamocortical terminals were seen in layers 1, 4, and 6 of the secondary AC and dorsoposterior AC, which coincided with labeled layer 6 cell bodies. Notably, after MGBd injection, a substantial number of layer 5 cells were labeled in all AC areas, whereas very few were seen after MGBv injection. Further, the degree of anterograde label in layer 4 of cortical columns containing labeled layer 6 cell bodies was greater than in columns containing labeled layer 5 cell bodies. These data suggest that auditory layer 5 corticothalamic projections are targeted to the MGBd in a nonreciprocal fashion and that the MGBd may route this information to the nonprimary AC. *J. Comp. Neurol.* 507:1209–1227, 2008.

© 2008 Wiley-Liss, Inc.

Indexing terms: thalamus; cortex; medial geniculate body; layer; driver; modulator

Thalamic nuclei can be divided into two categories: first order (FO) nuclei relay information from the periphery to the cortex, and higher order (HO) nuclei relay information from one cortical area to another (Guillery, 1995; Sherman and Guillery, 2002). This organizational scheme rests on the assumption that higher order thalamic nuclei bear a nonreciprocal relationship with two cortical areas. Although 30 years of studies involving bulk labeling and/or lesioning of either the thalamus or the cortex have concluded that there is general reciprocity in thalamocortical and corticothalamic projections (Diamond et al., 1969; Pontes et al., 1975; Robertson, 1977; Nelson and Kaas, 1981; Berson and Graybiel, 1983; Krubitzer and Kaas, 1987; Vaudano et al., 1991), suggesting a feedback role for corticothalamic projections, most of this work did not parse out these projections based on cortical layer of origin or termination type.

More recent work has revealed heterogeneity in the corticothalamic projection systems such that layer 5 neurons project to higher order thalamic nuclei, end in large

terminals on proximal dendrites, and show the physiological hallmarks of “driver” synapses (large excitatory postsynaptic potentials [EPSPs], ionotropic but not metabotropic glutamate receptor activation, paired-pulse depression), whereas layer 6 neurons project to higher and first order nuclei, end in small terminals on distal dendrites, and have the physiological characteristics of “modulator” synapses (small EPSPs, paired-pulse facilitation, metabotropic and ionotropic glutamate receptor activation; Mathers, 1972; Bourassa and Deschenes, 1995;

Grant sponsor: U.S. Public Health Service; Grant numbers: DC008320 (to D.A.L.), DC008794 (to S.M.S.), and EY003038 (to S.M.S.).

*Correspondence to: Daniel A. Llano, Department of Neurology, University of Chicago, 5841 S. Maryland, MC 2030, Chicago, IL 60637. E-mail: llano@uchicago.edu

Received 30 July 2007; Revised 9 November 2007; 13 November 2007

DOI 10.1002/cne.21602

Published online in Wiley InterScience (www.interscience.wiley.com).

Bourassa et al., 1995; Li et al., 2003; Reichova and Sherman, 2004; for a discussion of drivers vs. modulators, see Sherman and Guillery, 1998). These data suggest that layer 5 projections are endowed with the anatomic and physiologic properties necessary to serve a feedforward role in a cortico-thalamo-cortical circuit, whereas layer 6 modulator projections may be more suited to provide feedback modulation.

The mammalian auditory cortex (AC) contains multiple regions that have been organized into a quasi-hierarchical scheme based on the complexities of individual neurons' receptive fields and their intracortical connectivity (Rouiller et al., 1991). At the bottom of this hierarchy are the primary AC (AI) and the anterior auditory field (AAF), which are tonotopically organized, respond to sound at short latencies, and have relatively simple frequency receptive fields (hence "lemniscal"; Merzenich et al., 1975; Sally and Kelly, 1988; Thomas et al., 1993; Steibler et al., 1997). In rodents, there are at least two higher order regions, the secondary AC (AII) and a dorsoposterior region (DP in mouse, or TE2d in rat), both of which have weak tonotopy and complex frequency receptive fields (hence "nonlemniscal"; Sally and Kelly, 1988; Thomas and Tillein, 1997; Steibler et al., 1997). This difference is reflected in the medial geniculate body (MGB), such that the ventral division of the MGB (MGBv) provides the bulk of the thalamic input to the AAF and AI and has typical lemniscal response properties, whereas the dorsal MGB (MGBd) provides input to the DP and AII and has nonlemniscal response properties (Calford, 1983; Roger and Arnault, 1989; Arnault and Roger, 1990; Bordi and LeDoux, 1994a,b; Llano and Feng, 1999; Kimura et al., 2003).

Although several models have been proposed to account for the roles of the lemniscal and nonlemniscal auditory forebrain, the presence of large, driver-type terminals, found in the MGBd after AI tracer injections (Rouiller and Welker, 1991; Ojima, 1994; Bajo, 1995; Winer et al., 1999; Hazama et al., 2004), suggests that the early stages of cortical processing may involve a cortico-thalamo-cortical pathway, with the MGBd acting as a higher order relay, routing information from the AI to either the AII or DP. Therefore, the goal of the current study was to test two related hypotheses. First, the MGBd receives nonreciprocal driver-type input from layer 5 of AI, which would suggest a feedforward role for these projections. Second, the layer 6 input from the AC is organized in a reciprocal fashion with the MGB, implying a feedback role.

MATERIALS AND METHODS

Adult (60-day) Balb/c mice of both sexes were used for this study. All surgical procedures were approved by the Institutional Animal Care and Use Committee at the University of Chicago, and animals were housed in animal care facilities approved by the American Association for Accreditation of Laboratory Animal Care (AAALAC). Every attempt was made to minimize the number of animals used and to reduce suffering at all stages of the study. Mice were anesthetized with ketamine hydrochloride (100 mg/kg) and xylazine (3 mg/kg) and placed in a stereotaxic apparatus. Aseptic conditions were maintained throughout the surgery. Response to toe pinch was monitored, and supplements of anesthesia were administered when needed. Injection targets were localized by using stereotaxic coordinates (Paxinos and Franklin, 2001), and the penetration of specific targets were later confirmed by using cyto- and chemoarchitectural criteria (see below).

Micropipettes (tip diameter 10 μm) were filled with a solution of 5% biotinylated dextran amine (BDA; Molecular Probes, Eugene, OR) in phosphate-buffered saline (PBS; in all cases at pH 7.4), either 3,000 MW (MGB injections) or 10,000 MW (AC injections). For cortical injections, the electrode penetrated at approximately 40 degrees from the midline in the coronal plane and was lowered to about 800 μm from the surface. For MGB injections, the direction of penetration was parallel to the sagittal plane. BDA was ejected via iontophoresis by using current pulses of 5–10 μA , 7 seconds' duration, half-duty cycle for 10–15 minutes with negative current of the same amplitude pulsed as the electrode was passed through nontarget zones. The electrode remained in place for 5–10 minutes after each injection to minimize tracking of tracer up the electrode path. Injections were made bilaterally because there is no evidence to suggest that auditory thalamocortical or corticothalamic projections cross the midline (Bartlett et al., 2000).

Tissue processing

Animals were allowed to survive for 72 hours post injection and were then deeply anesthetized with ketamine and xylazine and perfused transcardially with 4% paraformaldehyde in PBS. The brains were postfixed overnight in perfusate. Brains destined for light microscopy were then placed in an ascending sucrose gradient for cryoprotection until saturated with 30% sucrose in PBS. Sixty- μm -thick sections were cut by using a sliding microtome and were exposed to 0.5% hydrogen peroxide for 30 minutes to quench endogenous peroxidases, washed three times in PBS, and then immersed in 0.3% (light microscopy) Triton-X (Sigma, St. Louis, MO) to enhance membrane permeability. Sections were then incubated for 4 hours at room temperature with peroxidase-based ABC reagent (Vectastain Elite ABC-Peroxidase Kit, Vector, Burlingame, CA), and washed in PBS, followed by two washes in Tris-buffered saline at pH 8.0. Visualization of label was done by using a cobalt-intensified, diaminobenzidine (DAB) reaction (SigmaFast tablets).

Alternate sections were taken for either immunostaining, Nissl staining or, in one case, for cytochrome oxidase staining. For immunohistochemistry, sections were placed in 0.5% H_2O_2 for 30 minutes, rinsed in PBS, and then incubated for 30 minutes in PBS containing 0.3% Triton-X, followed by 1.5% normal horse serum (NHS);

Abbreviations

AC	auditory cortex
AAF	anterior auditory field
AI	primary auditory cortex
AII	secondary auditory cortex
D	dorsal
DP	dorsoposterior region
LP	lateral posterior nucleus
LGN	lateral geniculate nucleus
M	medial
MGB	medial geniculate body
MGBd	dorsal MGB
MGBm	medial MGB
MGBv	ventral MGB
MGMz	marginal zone of the MGB
PP	peripeduncular area
RF	rhinal fissure

Vector) in 0.3% Triton-X for 30 minutes. Sections were then incubated at 4°C overnight in a primary antibody solution (1:2,000 for both anti-calbindin and anti-parvalbumin monoclonal antibodies; Sigma) in 1.5% NHS and 0.3% Triton-X, followed by 1 hour in a 1:200 dilution of peroxidase-labeled anti-mouse secondary antibody made in horse (Vector) solution in 1.5% NHS and 0.3% Triton-X. Peroxidase was visualized by using either cobalt-intensified DAB (as above), or non-cobalt-intensified DAB (SigmaFast tablets) when sections were processed for both BDA and calcium-binding protein immunohistochemistry. Nissl staining was done by using standard procedures on mounted sections using either cresyl violet (0.5%) or neutral red (1%, when the same sections were processed for BDA). For cytochrome oxidase staining, the method of Wong-Riley (1979) was used. Sections were incubated with a solution of 0.05% DAB, 4% sucrose, and 20% cytochrome C (Sigma) in PBS in the dark at 37°C for 4 hours and quenched with PBS. All sections were mounted on gelatin-coated slides, air-dried, and coverslipped by using Permount. All images were taken from either a Zeiss axiocam digital camera or a Retiga 2000 monochrome CCD camera mounted to a Leitz Wetzlar Orthoplan microscope or a Leica DM5000 microscope, respectively.

Images were captured by using Axiovision software (for the Zeiss camera) or Q Capture Pro software (for the Retiga camera). The images were imported into Powerpoint or CorelDraw for final preparation and for adjustment of contrast and brightness. All images had brightness and contrast adjusted to bring out notable features or to match image brightness for montage preparation. However, no focal editing or focal changes in brightness or contrast were made.

Antibody specificity

Our parvalbumin monoclonal antibody (Sigma, product number P 3008, clone PARV-19, lot number 064K4777) was generated against purified frog muscle parvalbumin. Per the manufacturer, this antibody does not react with other members of the EF-hand family, such as calmodulin, intestinal calcium-binding protein, S100A2 (S100L), S100A6 (calyculin), the α -chain of S-100 or the β -chain (in S100a and S-100b), myosin light chain, or troponin. Each lot is tested by using an immunoblot with rabbit skeletal muscle extract as antigen and yields a single band at 12 kDa. Our calbindin monoclonal antibody (Sigma, product number C9848, lot number CB016K4786) was generated against purified bovine kidney calbindin D-28k. Per the manufacturer, this monoclonal antibody does not react with other members of the EF-hand family such as calbindin-D-9K, calretinin, myosin light chain, parvalbumin, S-100a, S-100b, S100A2 (S100L), or S100A6 (calyculin). Each lot is tested by using an immunoblot with bovine kidney cell extract as antigen and yields a single band at 28 kDa. We have eliminated the primary antibody for both calbindin and parvalbumin in control experiments, and this has shown no staining (data not shown). In addition, the patterns of staining that we observed for calbindin and parvalbumin (see Figs. 1C,D) is virtually identical to that demonstrated in the mouse (Cruikshank et al., 2001) and is very similar to the patterns seen in the rabbit and monkey (Hashikawa et al., 1991; de Venecia et al., 1995).

Data analysis

Injection sites were assigned a location within the AC or MGB based on the cytoarchitectural and chemoarchitectonic (calbindin or parvalbumin immunostaining) criteria described below. Injection volumes, not corrected for tissue shrinkage, were determined by multiplying the cross-sectional area of the injection site seen on each section by 50 μ m, and then by 2 (to account for alternate sections) or 3 (when every third section was stained for BDA, and the others were immuno- or Nissl-stained). We have adopted the nomenclature of Stiebler and others (Stiebler, 1987; Stiebler et al., 1997) for the mouse AC, which is parcelated into two lemniscal tonotopic regions (AI and AAF), as well as two nonlemniscal, weakly tonotopic regions (DP, AII). We have not distinguished between the ultrasonic field and AI and AAF because a clear cyto- or chemoarchitectural description of this area has yet to be published and because this area has some elements of both lemniscal AC areas (i.e., it receives input from the MGBv; Hoffstetter and Ehret, 1992) and nonlemniscal AC areas (it is not tonotopic; Stiebler et al., 1997).

Based on work in the mouse AC (Caviness, 1975; Wree et al., 1983; Stiebler et al., 1997; Cruikshank et al., 2001), and by its homology to the rat (Arnault and Roger, 1990; Shi and Cassell, 1997; Hazama et al., 2004) and gerbil (Budinger et al., 2000a), we have defined the AAF and AI by their koniocellular architecture and their greater thickness than the AII, which is thin and agranular (Fig. 1B). In addition, both the AI and AAF have been shown to have strong parvalbumin immunoreactivity, whereas the AII, by contrast, has virtually no staining for parvalbumin (Wallace et al., 1991; Molinari et al., 1995; Budinger et al., 2000a; Cruikshank et al., 2001). We distinguished the AAF from the AI by their rostrocaudal positions. (The AI is 3.2–3.8 mm posterior to bregma, whereas the AAF is 2.6–3.2 mm posterior to bregma.) To define the DP, we have used its homology to TE2d in the rat, its identity as a nontonotopic hypogranular auditory cortical region that receives input from the MGBd, and its dorsocaudal position with respect to the AI (Arnault and Roger, 1990; Shi and Cassell, 1997; Hazama et al., 2004; Donishi et al., 2006). This area likely corresponds to mouse cortical area 22, which has been described by Caviness (1975) as being thinner, with less dense cellularity in layers 4 and 5. We have used standard nomenclature for the three major subdivisions of the MGB (the ventral, dorsal, and medial divisions of this thalamic nucleus) and utilized the nomenclature of Clerici and Coleman (1990) for the rat MGB when referring to subnuclei within the dorsal and ventral divisions. The subnuclei for the dorsal division are the suprageniculata, dorsocaudal, dorsal, and deep dorsal; and for the ventral division are the ovoid nucleus, lateral ventral, and MG marginal zone.

Corticothalamic terminals were assigned a category based on Guillery's classification system for light-level observations of afferent terminals to the thalamus (Guillery, 1966). In this system, type I axons are slender and give off multiple, small, synaptic "knobs" along their course. Type II axons tend to be thicker and give off large, clustered, flower-like arrangements of large terminals. Type I and type II terminals likely correspond to the round-vesicle, small-terminal (RS) and round-vesicle, large-terminal (RL) types, respectively, that are seen at

the ultrastructural level in the corticopulvinar system (Mathers, 1972).

We have modified this classification system to include only a single parameter, long-axis length of the terminal, which has been shown to delineate separate populations of corticopulvinar terminals in the cat (Van Horn and Sherman, 2004). All sections were systematically examined at 100 \times (Leica N-plan, NA 1.25) with a calibrated eyepiece. For assessment of distribution of terminal size, single sections of the MGB containing a high density of corticothalamic staining were selected. The long-axis length of all terminals (up to 100 terminals) in the full 60- μm depth of either one (for the MGBv) or two 10,000 μm^2 squares were measured. Two squares were used in 2/3 MGBd sections to increase the number of terminals analyzed. Note that the goal of the analysis was not to assess the density of terminal staining (unlike subsequent analysis; see below) but to amass enough terminals for analysis of the distribution of terminal sizes. Measurements were done by using ImageJ software (<http://rsb.info.nih.gov/ij/>). Terminals with length less than 0.3 μm , were binned into a single bin of less than 0.3 μm , given the limits of the resolution at the light microscopic level with this combination of magnification and numerical aperture (Slaytor, 1970).

To assess the spatial distribution of terminal types, all sections were systematically examined at 100 \times to look for terminals greater than 1–2 μm in long-axis length. All such terminals were then photographed and had their long axes remeasured via Axiovision software. Care was taken to exclude terminals with greater than two feeding axons because it is impossible to resolve whether or not such “terminals” represent an individual terminal or several overlapping terminals. All terminals greater than 2 μm in long axis were called *type II*; all others were *type I*. All type II terminals and retrogradely labeled cell bodies were plotted on a high-resolution blowup of the MGB using local landmarks for further analysis. For type I terminal counts in the MGB, a grid with 100- μm spacing was placed over computerized images from the MGB, and each animal, section, and each square on each grid were assigned a number. A random number generator was used to pick numbered sites in the ventral or MGBd for counting. Once a site was found, all type I terminals in the full depth of a 100 \times 100- μm square were counted at 40 \times by using a calibrated eyepiece. To avoid double counts, all counting started from the center of each square and progressed in a counterclockwise fashion. A similar procedure was used for synaptic counts in the cortex.

Statistics

All synaptic counts were treated as independent samples, and thus a Student's *t*-test was used to compare the distributions and compute significance. For all categorical data (e.g., laminar or sublaminar distribution of corticothalamic projections), 2 \times 2 tables were constructed to compute Chi-squared values. A Mann-Whitney U-test was used to compare the distributions of long-axis lengths of terminals from the MGBv and MGBd, given their nongaussian distribution in the MGBd (see Fig. 3).

RESULTS

Subdivisions of the AC and MGB

Nissl staining of the AC revealed prominent differences in cytoarchitecture corresponding to the previously described borders between the lemniscal and nonlemniscal AC. As shown in Figure 1B, the AI demonstrates prominent lamination with dense granularity within layer 4, whereas the AII is thinner, with a frankly agranular organization (Fig. 1B). The AAF demonstrates a lamination pattern similar to that of the AI (not shown). As described in Materials and Methods, we have used Caviness's (1975) description of area 22 to define the DP, which is also thinner and less granular than the AI but retains greater lamination than the AII. We found strong immunostaining for parvalbumin in nonpyramidal cells of layers 2/3 and 5 of the AI, AAF, and DP, virtually no staining for parvalbumin in the AII (Fig. 1D,F), and a slight prominence of cytochrome oxidase signal in the AI, relative to the AII, as described previously (Gonzalez-Lima and Cada, 1994). We found no differences in calbindin staining in any AC area.

Nissl and immunostaining of the MGB revealed differences among the subdivisions consistent with previous descriptions (Fig. 1A,C,D; Morest, 1965; Clerici and Coleman, 1990; Molinari et al., 1995; Budinger et al., 2000b; Cruikshank et al., 2001). The MGBv is characterized by densely packed small cells. In the lateral portions of the MGBv, cells were packed in arrays oriented from dorsolateral to ventromedial, whereas in the more medial portions, the cell packing was organized in concentric circles, although this distinction was not apparent in all sections. These differences likely correspond to the lateral ventral and ovoid nuclei of the MGBv, respectively. The MGBv also showed strong neuropil staining and moderate somatic staining for parvalbumin, with no calbindin staining. The MGBd had large cell bodies, particularly in the most dorsal and medial portions, with no obvious packing arrangement to the cells. The largest cells in the medial portions of the MGBd formed their own structure within the MGBd, likely corresponding to the supragenulate nucleus, but this was not obvious on all sections. The MGBd showed strong somatic staining for calbindin and weak staining for parvalbumin, primarily in the neuropil. The medial division of the MGB (MGBm) in general showed a loose packing arrangement, with some very large cells. Similar to the MGBd, the MGBm had strong somatic staining for calbindin and weak neuropil staining for parvalbumin. In general, the differences in immunostaining patterns between the MGBd and MGBv were obvious but did not distinguish subnuclei within the MGBv and MGBd. In addition, the differences in the subnuclei were not always apparent using Nissl stains. Thus no attempt was made in this study to delineate the projection patterns of the subnuclei of the MGBd and MGBv.

Summary of injections

There were six injections of 10,000 kDa MW BDA into either the AI (four injections) or the AAF (two injections). An example of a typical injection site on a flattened cortex, counterstained for cytochrome oxidase (to illustrate the position of the barrel cortex) or for parvalbumin, is shown in Figure 1E and F, respectively. The mean injection maximum cross-sectional area (uncorrected for tissue shrinkage) was $2.5 \times 10^5 \mu\text{m}^2$ (SD $1.1 \times 10^5 \mu\text{m}^2$), and the

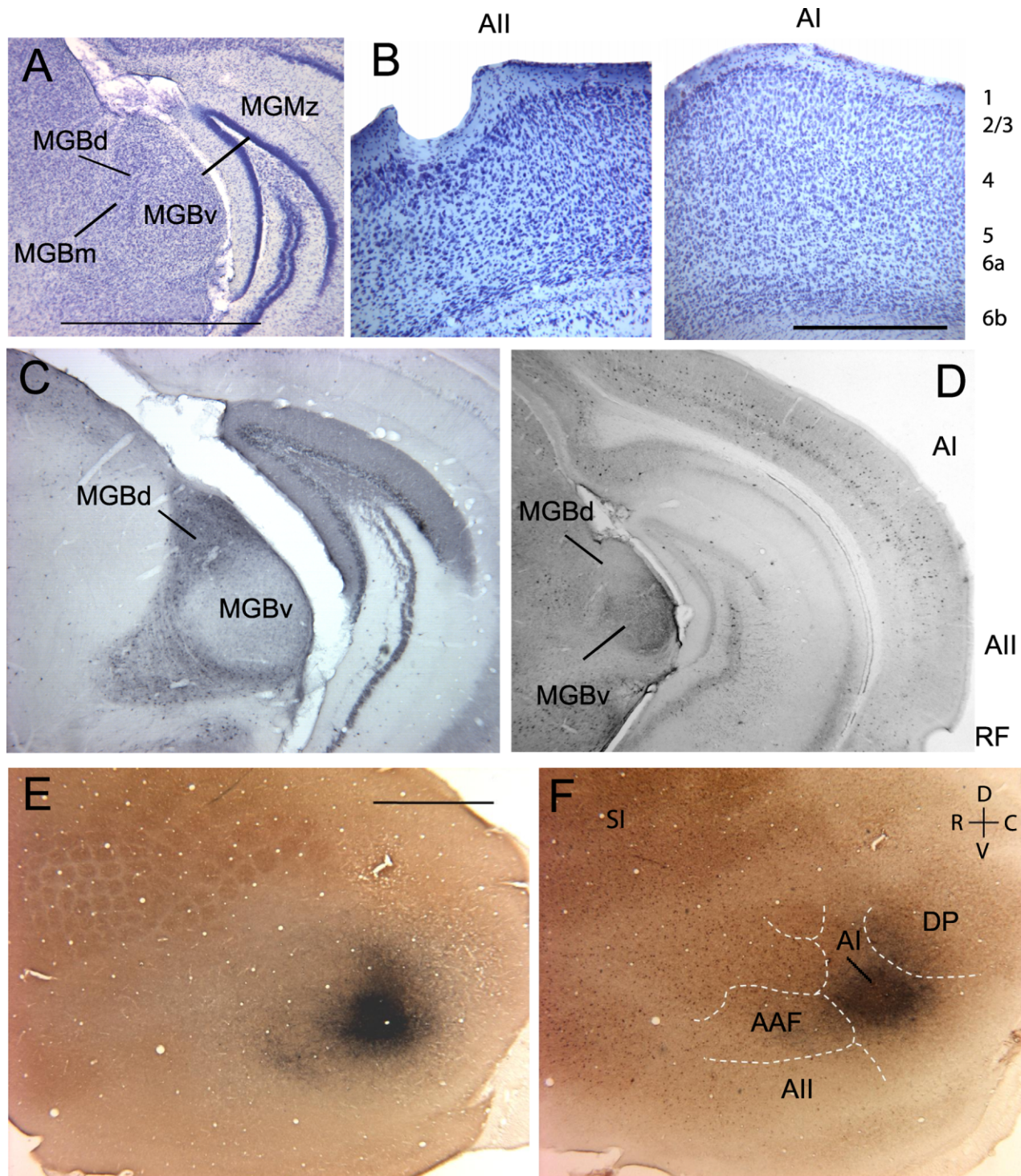


Fig. 1. **A:** Cresyl violet-stained coronal section through the MGB illustrating the three major subdivisions of the MGB (the MGBv, MGBd, and MGBm), as well as the marginal zone of the MGB (MGMz). **B:** Cresyl violet-stained coronal sections through the AI and AII illustrating the increased thickness and granularity of the AI compared with the AII. **C,D:** Calbindin- and parvalbumin-

immunostained coronal sections, respectively. **E,F:** Flat mounts of mouse neocortex, demonstrating an injection site into the AI and counterstained for cytochrome oxidase (**E**) or immunostained for parvalbumin (**F**). Superimposed on the cortex is the map of the mouse AC proposed by Stiebler (1987). For abbreviations, see list. Scale bar = 1 mm in A (applies to A,C,D) and E (applies to E,F); 500 μ m in B.

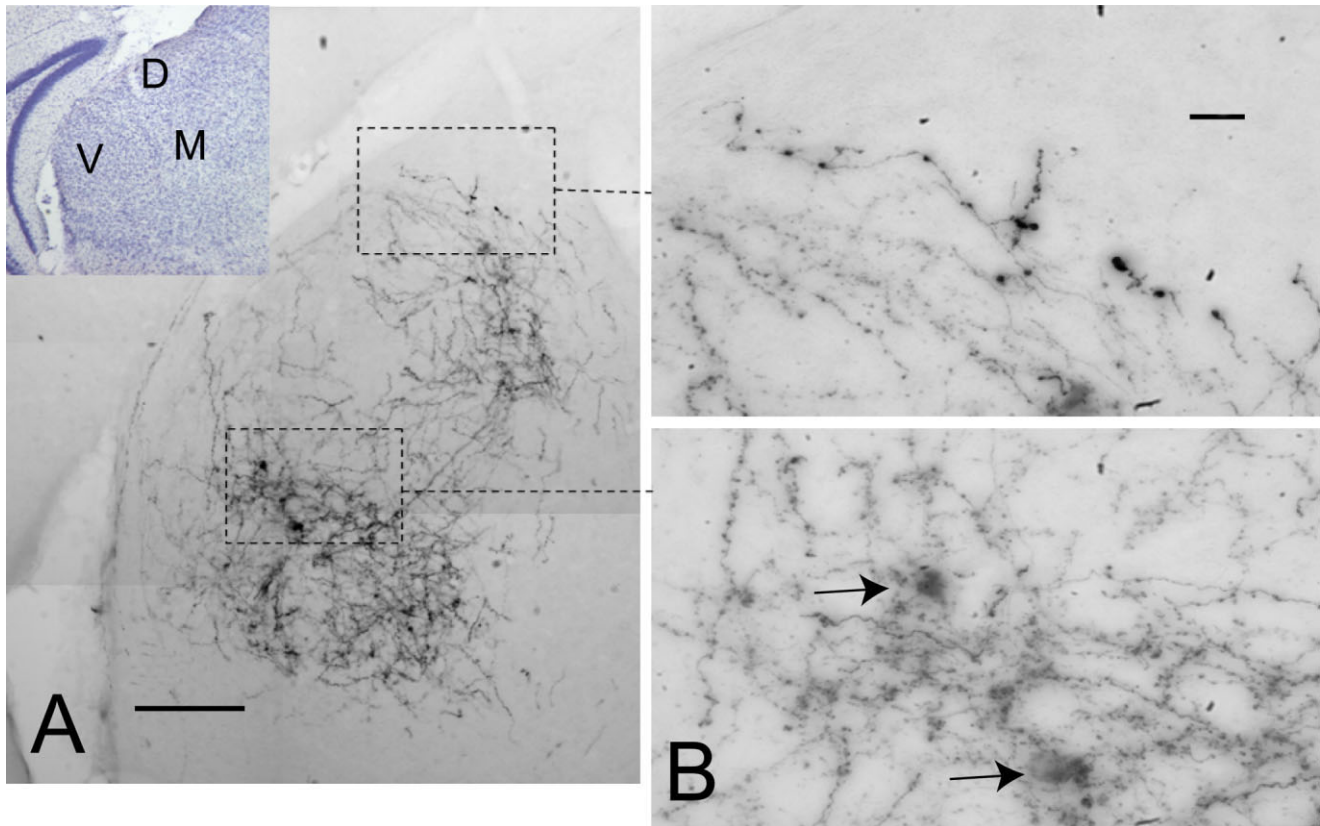


Fig. 2. **A:** Photomontage of the MGB after injection of BDA into the AI. **Inset:** An alternate section, stained with cresyl violet, to illustrate the subdivisions of the MGB (D, MGBd; V, MGBv; M, MGBm). **B:** Expanded areas from the MGBv and MGBd optically reconstructed at 40 \times showing a cluster of type II terminals (top) and

type I terminals with two retrogradely labeled thalamocortical cell bodies (bottom). Arrows indicate retrogradely labeled cell bodies in the MGBv. For abbreviations, see list. Scale bar = 200 μm in A; 20 μm in B.

injections were centered in layers 4–6 (as determined by comparison with alternate Nissl-stained sections), although in all the cases there was spread of label to the supragranular layers. In the MGB, two injections of 3,000 kDa MW BDA were made into the MGBv (mean injection maximum cross-sectional area = $0.77 \times 10^5 \mu\text{m}^2$) and three injections into the MGBd (mean injection maximum cross-sectional area = $0.40 \times 10^5 \mu\text{m}^2$).

Cortex injections

AI and AAF injections produced intense anterograde staining in one or two large bands in the MGBv, one oriented dorsolaterally to ventromedially and often an additional horizontal band at the dorsal edge of the MGBv (Fig. 2A). There was also lighter axonal and terminal staining throughout the rest of the MGBv and sparse staining in the MGBd and MGBm. Under high magnification, we discerned that the large bands of label were comprised of highly branched small axons studded with multiple branches ending in small synaptic terminals ($<1 \mu\text{m}$ in long-axis diameter), which we call type I terminals (Guillery, 1966). Anterograde corticothalamic labeling in the MGBd consisted of a small number of type I terminals as well as thick axons, ending in large terminals ($>2 \mu\text{m}$), which we call type II terminals (also based on Guillery, 1966). Type II terminals tended to be found in clusters of

four to five and emanated from large axons with a relatively small number of branches (Fig. 2B, upper half). Dense terminal labeling was also seen in the auditory portion of the thalamic reticular nucleus (not shown). Retrograde labeling of thalamocortical relay neurons was relatively sparse but almost exclusively found in the MGBv and coincided with areas of dense type I terminals (Fig. 2B, lower half). Most neurons showed dense granular labeling, clearly delineating the outline of somata, with filling only to the proximal dendrites.

Terminal sizes were analyzed by measuring their long-axis length. The distributions of long-axis length in the MGBd and the MGBv, pooled from the first three injection sites studied, is shown in Figure 3. The distribution of terminal sizes in the MGBv appeared to have a normal distribution (with slight skewing at the short-length end, given the resolution limits of our approach; Slaytor, 1970). A similar peak was seen in the MGBd (although in much smaller numbers). In addition, there was a second peak in the MGBd at long-axis lengths greater than 2.0 μm . The difference between the distribution of terminal sizes in the MGBd and MGBv was significantly different ($P < 0.001$, $U = 24571.0$, Mann-Whitney test). Given these data, a conservative estimate of 2 μm was used for subsequent analysis to score a terminal at the light microscopic level as being type I ($<2.0 \mu\text{m}$) or type II ($>2.0 \mu\text{m}$; see below).

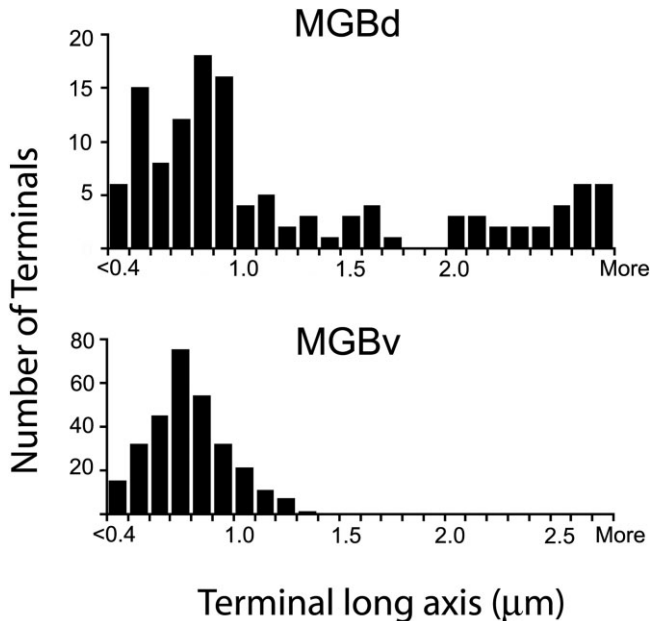


Fig. 3. Distributions of long-axis lengths of terminals in the MGBd (A) and MGBv (B). Bin size = 0.1 μm , except for the first bin, which is 0.3 μm and under, given the resolution limitations at the light microscopic level. Data are pooled over three animals. $n = 126$ for MGBd; $n = 293$ for MGBv. For abbreviations, see list.

Type II terminals were located primarily in the MGBd and were segregated from retrogradely labeled thalamic relay cells. An example of the distribution of type II terminals and labeled relay cell bodies is shown in Figure 4. Type II terminals were found throughout the rostrocaudal extent of the MGB, but primarily in the MGBd, with occasional large terminals in the peripeduncular area and the MGBm, including its marginal zone (asterisk in Fig. 4). In this example, cell bodies were found exclusively in the MGBv, overlapping the major extent of the anterograde small terminal (type I) labeling. As shown in Figure 5, across all six animals, the type II terminals were distributed primarily in the MGBd and MGBm. The labeled relay cell bodies were in the MGBv, and these were found in regions of dense small-terminal (type I) labeling. Again, a few large (type II) terminals were found in the peripeduncular area. We emphasize that the distribution of type II terminals and retrogradely labeled relay cell bodies was segregated, with type II terminals chiefly in the MGBd and relay cell bodies primarily in the MGBv, with the exception of the caudalmost portion of the MGBm, where they were intermixed (Fig. 5, caudalmost section; see Discussion), thus demonstrating a lack of corticothalamic and thalamocortical reciprocity with respect to the large-terminal (type II) system.

Labeled type I terminals were heavily distributed in dense bands across the MGBv, presumably reflecting the tonotopic location of the AC injection site relative to the known tonotopic laminar arrangement within the MGBv (Morel et al., 1987; Redies and Bradner, 1991). The density of type I terminal innervation was higher in the MGBv than in the MGBd, as assessed by comparison of terminal density in these divisions. A total of 20 locations (10 in the MGBv and 10 in the MGBd) were chosen at

random from $100 \times 100\text{-}\mu\text{m}$ grids that were placed over the MGB. The density of type I terminal labeling in the grids in the MGBv was 334 terminals/ $10,000 \mu\text{m}^2$ (SD 239 terminals/ $10,000 \mu\text{m}^2$) vs. 24.2 terminals/ $10,000 \mu\text{m}^2$ (SD 19 terminals/ $10,000 \mu\text{m}^2$) in the MGBd ($P < 0.001$, Student's *t*-test). Thus the densest type I terminal labeling overlapped the retrograde labeling of relay cells, and this further indicates strong reciprocity of thalamocortical and type I corticothalamic pathways to and from the MGBv. Note that the difference in type I terminal density between the MGBd and MGBv differs in this analysis from the analysis seen in Figure 3. This is because of the difference in sampling used for the two approaches. The current approach used random sampling of grid points, in which in some cases, the terminal density was very low. For Figure 3, sections that had high density of anterograde labeling were selected (see Materials and Methods) in order to acquire enough terminals (particularly in the MGBd, where labeling density is low) to assess their distribution.

Thalamus injections

Injection of 3,000 MW BDA into the MGBv produced two regions of dense anterograde and retrograde label in the AC. Both regions were located in the koniocellular portion of the temporal cortex. One region was displaced anteriorly and slightly ventrally to the other. (Total rostral-caudal extent of label was from 2.5 to 3.8 mm posterior to bregma.) Based on these characteristics, these areas corresponded to the AI (posterior dorsal region) and AAF (anteroventral region). No label was observed in the AII or DP. Dense terminal and retrograde somatic labeling was seen in the auditory portion of the thalamic reticular nucleus, and scattered retrograde labeling was seen across the central nucleus of the inferior colliculus of both animals (not shown). An example of the cortical labeling following injections into the MGBv is shown in Figure 6B (injection site in Fig. 6A). In both the AAF and AI, there was dense terminal labeling in layers 4 and 6, with no terminal labeling in layer 1. Retrograde corticothalamic label was seen in all sublamina of layer 6. There was close correspondence between regions of anterograde and retrograde label, again suggesting reciprocity. The rostrocaudal extent of cortical label for this animal is shown in Figure 6C. Labeled layer 6 corticothalamic cell bodies were seen across the AI and AAF, corresponding closely to regions of anterograde layer 4 and 6 thalamocortical terminal labeling. A single layer 5 labeled neuron was found vs. a total of 119 layer 6 labeled neurons. The distributions of anterograde and retrograde label, as well as the proportions of labeled layer 5 and layer 6 corticothalamic neurons, was virtually identical in the second animal that was injected in the MGBv (1 layer 5 vs. 93 layer 6 labeled corticothalamic neurons).

Injection of 3,000 MW BDA into the MGBd labeled several cortical areas. In general, cortical labeling was less dense than with MGBv injections, likely related in part to the smaller injection size in our material. An example of the distribution of cortical labeling is shown in Figure 7B (injection site shown in Fig. 7A). Most anterograde labeling was seen in layers 1, 4, and 6 in both the AII and DP (dashed boxes), although lighter terminal labeling was seen in layers 1 and 6 of AI. Retrograde layer 6 corticothalamic label was seen primarily in the DP and AII (asterisks), although occasional labeled layer 6 cells

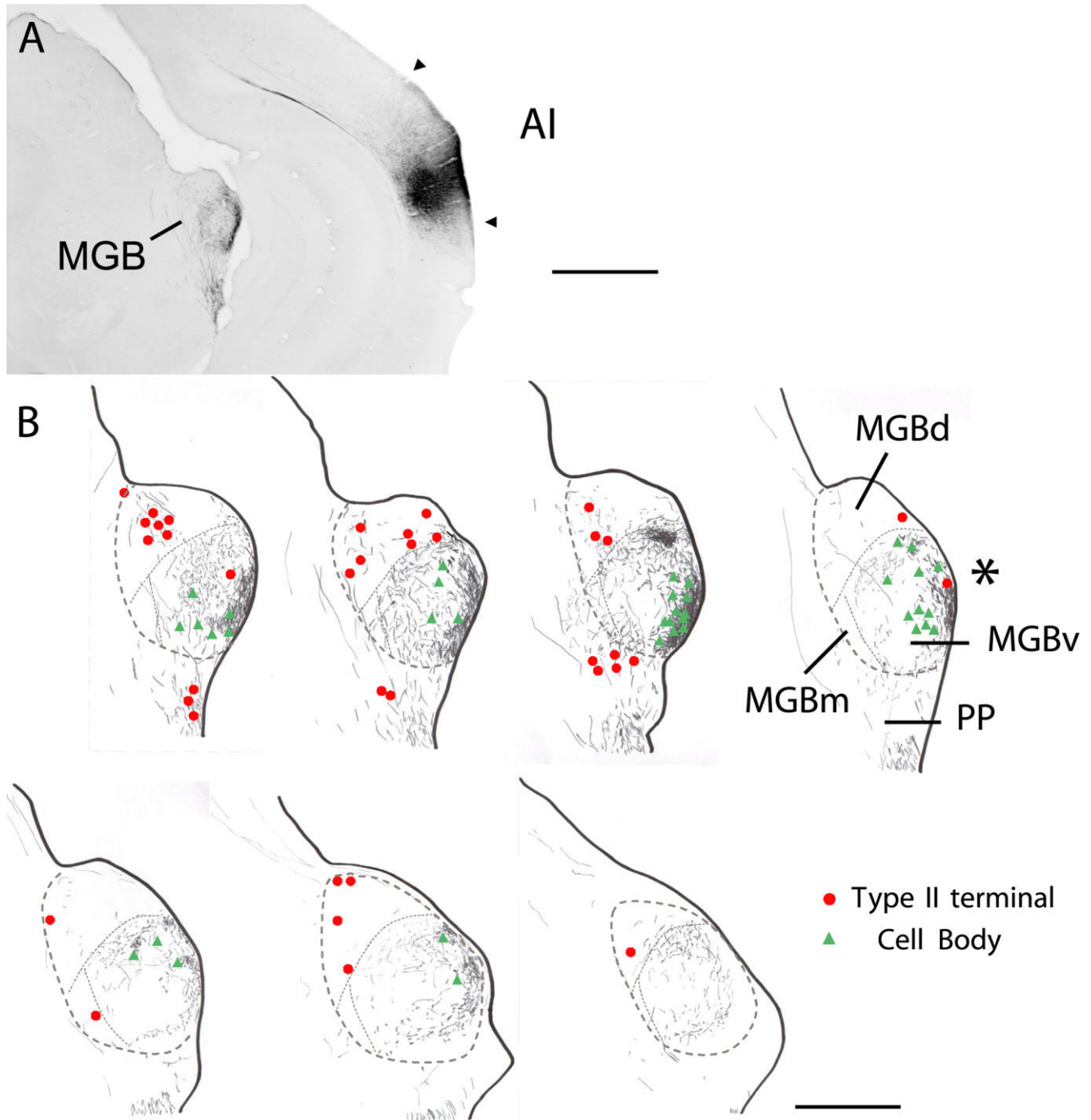


Fig. 4. Example of the distribution of type II terminals and retrogradely labeled cell bodies after injection of BDA into AI. **A:** Coronal section using metal-intensified DAB to visualize BDA, without counterstain, illustrating the injection site in the AI as well as the distribution of labeling in the MGB. **B:** Series of camera lucida reconstructions, from caudal to rostral, of the anterograde labeling in MGB,

overlaid with the locations of type II terminals (red circles) and retrogradely labeled thalamocortical cell bodies (green triangles). The asterisk represents a type II terminal found in the marginal zone of the MGB. Scale bar = 1 mm in A; 0.5 mm in B. For abbreviations, see list.

were seen in the AI. In addition, terminal and retrograde somatic labeling was seen in the auditory portion of the thalamic reticular nucleus, and scattered retrograde labeling was seen across the external nuclei of the inferior colliculus (not shown).

Layer 5 retrograde label was seen in both the AI and DP (red arrows). The distribution of anterograde and retrograde labeling across the cortex is shown in Figure 7C. As shown in Figure 7C, anterograde label and layer 6 retrograde label was primarily found in the nonlemniscal re-

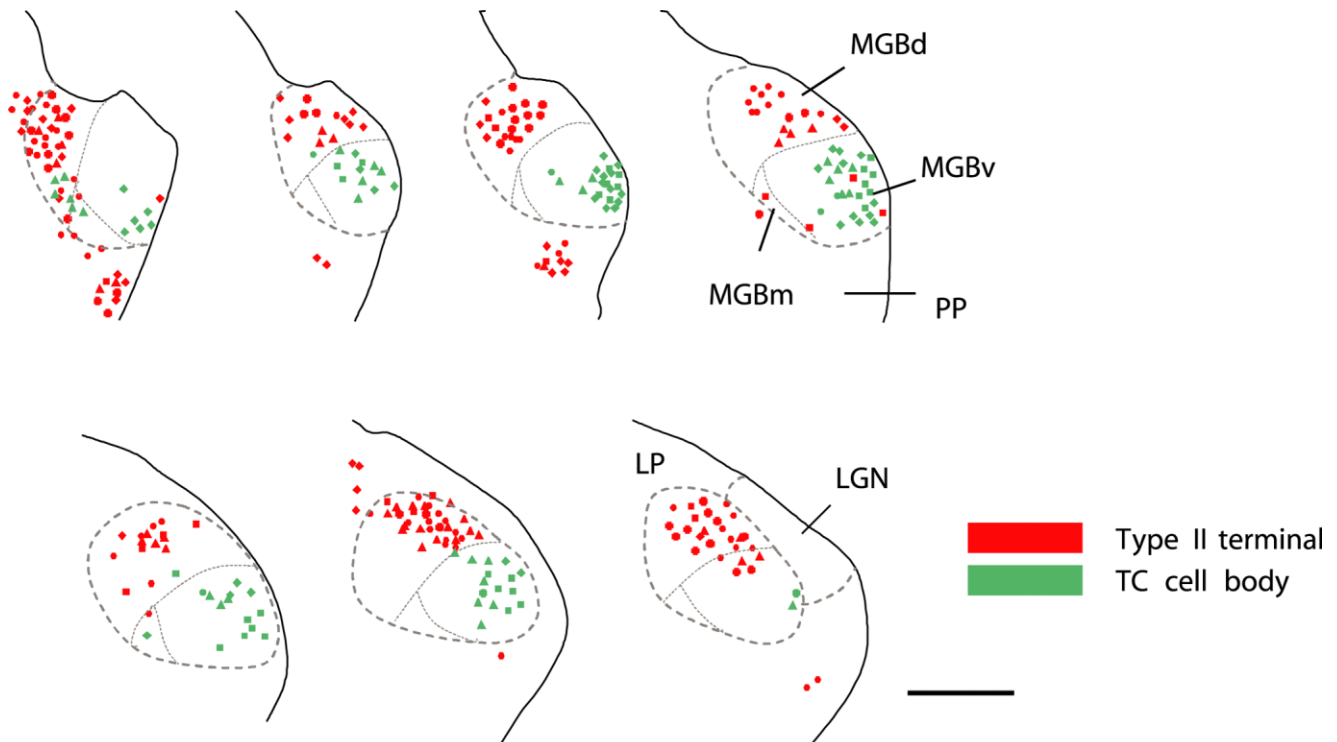


Fig. 5. Summary slide illustrating the distribution of type II terminals and retrogradely labeled thalamocortical cell bodies across the MGB, with data pooled from six different AI or AAF injections. Sections drawn from caudal to rostral. Circles, injection 8.11.06.2L;

squares, 9.12.06.2L; plus signs, 8.11.06.3L; diamonds, 9.12.06.2R; hexagons, 8.11.06.3R; triangles, 7.31.06.4R. Scale bar = 0.5 mm. For abbreviations, see list.

gions of the AC (DP and AII), whereas layer 5 retrograde label was distributed to both lemniscal and nonlemniscal regions. In addition, several layer 5 labeled cells were seen in the visual cortex, likely related to extension of the injection site into the lateral posterior nucleus because visual cortical labeling was not seen in the two other MGBd injections that did not extend to the lateral posterior nucleus.

Although the montage in Figure 7 was created to illustrate the spatial relationships among the DP, AI, and AII in the same section, anterograde labeling in the DP was denser in caudal sections (peak at -3.88 from mm bregma), whereas anterograde labeling in AII was denser in more rostral sections (peak at -2.18 mm from bregma). The anterograde label from these points is illustrated in Figure 8 to compare the distribution of thalamocortical label in the nonlemniscal vs. lemniscal AC. As shown, the highest density of thalamocortical input to all regions was to cortical layer 4, with a smaller component to layer 6. There is additional layer 1 projection in the nonlemniscal AC, which is not seen in the lemniscal AC. Also note the lack of anterograde label in layer 4 of the AI after MGBd injection, despite the presence of anterograde layer 1 and 6 label, as well as a retrogradely labeled layer 5 neuron (Fig. 8C).

The distribution of layer 5 and 6 corticothalamic label from all three MGBd injections is shown in Figure 9. This figure illustrates the dissociation of layer 6 and layer 5 input with respect to the lemniscal and non lemniscal AC.

Labeled layer 6 cells were primarily found in the nonlemniscal portions of the AC (DP and AII), whereas labeled layer 5 cells were primarily found in the lemniscal portions (AAF and AI). In addition, a larger percentage of labeled corticothalamic neurons emanated from layer 5 after injections of the MGBd than after injections of the MGBv (29/41 for the former compared with 2/214 for the latter, $DF = 1$, $\chi^2 = 157$, $P < 0.001$). Furthermore, there was a difference in the degree of reciprocity with the MGB vis à vis labeled layer 5 and layer 6 cells. Ten layer 5 and ten layer 6 labeled corticothalamic cells (after MGBd injections) were selected randomly from all areas of the AC, and the numbers of orthogradely labeled terminals in a 100×100 - μm^2 square centered in layer 4 above the selected cells were counted. The mean terminal densities were 233 terminals/ $10,000 \mu\text{m}^2$ (SD 154 terminals/ $10,000 \mu\text{m}^2$) above layer 6 corticothalamic cells vs. 30.1 terminals/ $10,000 \mu\text{m}^2$ (SD 65.2 terminals/ $10,000 \mu\text{m}^2$; $P < 0.001$, Student's *t*-test), suggesting that layer 6 corticothalamic neurons are found in regions receiving a higher degree of thalamocortical input than layer 5 corticothalamic neurons.

Sublaminar organization of layer 6 corticothalamic projections

The sublaminar pattern of labeled layer 6 neurons was also examined, as this has been found to differ in the lemniscal vs. nonlemniscal portions of the somatosensory corticothalamic projection (Zhang and Deschenes, 1997; Killackey and Sherman, 2003). Based on criteria of Zhang

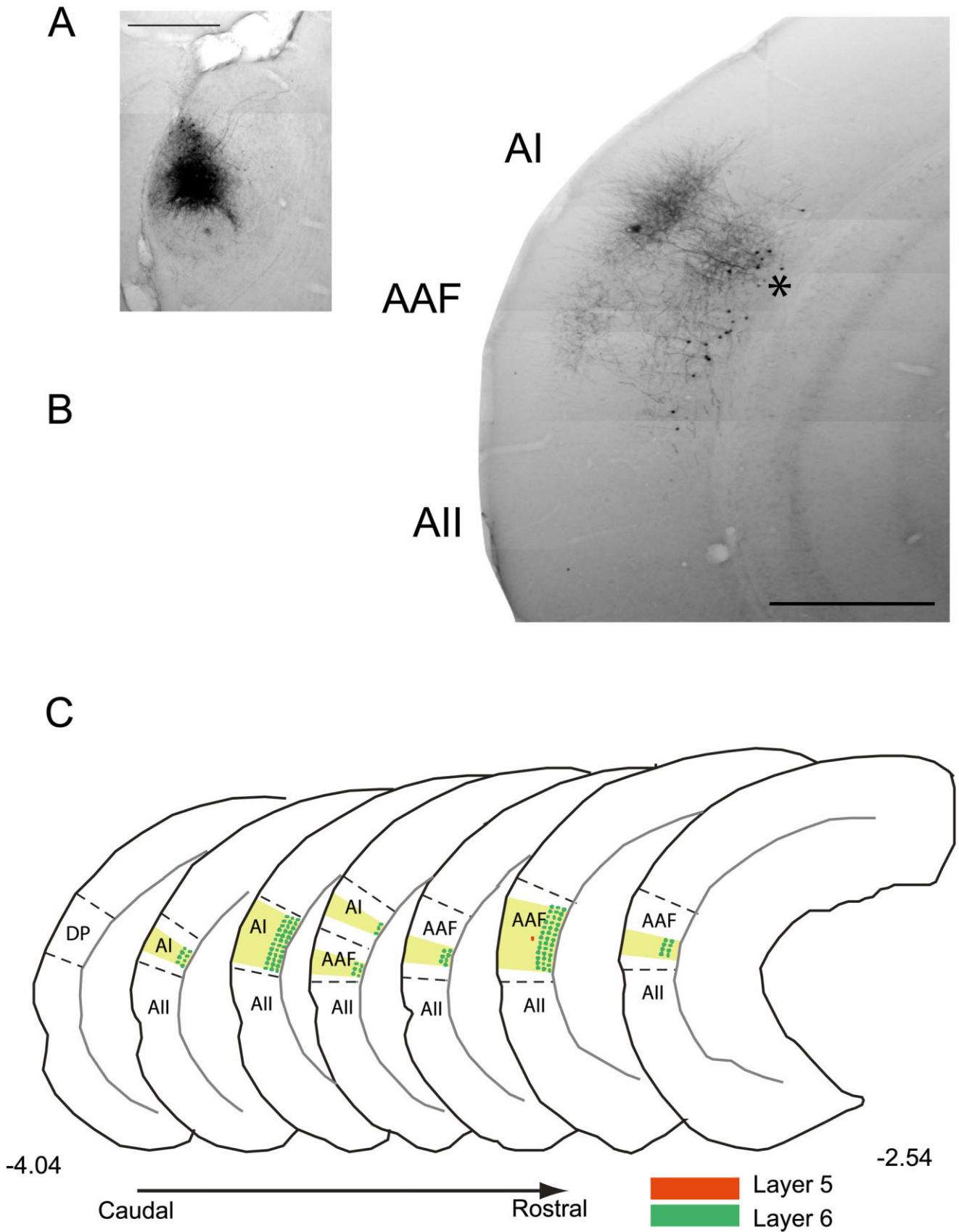


Fig. 6. **A:** Injection site illustrating an MGBv injection. **B:** Photomontage of the distribution of anterograde and retrograde label in the AC. Asterisk demonstrates a layer 6 retrogradely labeled corticothalamic cell body. **C:** Distribution of anterograde and retrograde label across the rostrocaudal extent of the cortex from the same injection site shown above, drawn onto tracings from Paxinos and Franklin

(2001). Yellow represents regions receiving major anterograde input. Green and red circles represent layer 6 and layer 5 corticothalamic cells, respectively. Numbers below represent the position of the sections relative to bregma. Scale bar = 500 μ m in A,B. For abbreviations, see list.

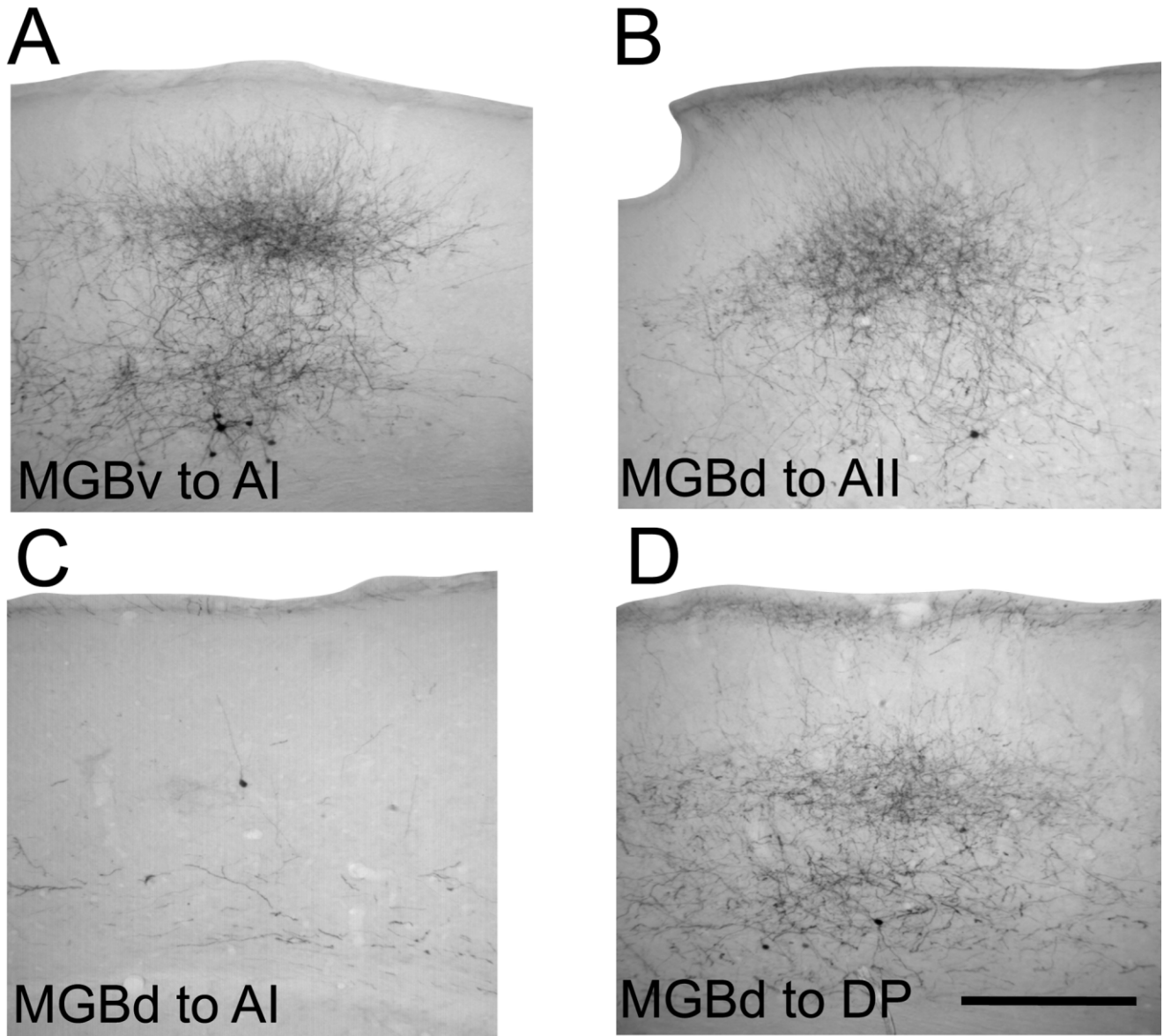


Fig. 8. Photographs demonstrating the distribution of thalamocortical anterograde label in several regions of cortex. **A:** MGBv to AI. **B:** MGBd to AII. **C:** MGBd to AI. **D:** MGBd to DP. Notice that in A, B, and D, there is major input to cortical layer 4, with less in layer 6.

There is an additional projection to layer 1 seen only in the nonlemniscal areas. Scale bar = 250 μ m in D (applies to A–D). For abbreviations, see list.

and Deschenes (1997), we divided layer 6 into two sublayers: layer 6a and layer 6b. Layer 6b is located within a band of tangentially traveling fibers and consists of densely packed small cells; it tends to occupy the lower 20% of layer 6. In our samples, for injections of the MGBd, 11/41 (27%) labeled layer 6 cells were in layer 6b, whereas after injections of the ventral division, 30/214 (14%) cells were in layer 6b ($P < 0.05$, via χ^2 comparison, $DF = 1$, $\chi^2 = 4.18$). This suggests that the sublaminar distribution of the layer 6 corticothalamic projection differs between the dorsal and ventral divisions of the MGB, namely, that the dorsal division receives a greater proportion of corticothalamic input from layer 6b.

DISCUSSION

Summary of findings

We utilized the driver/modulator dichotomy (see Introduction) to parse out the projections from the AC to MGB and compared their reciprocity with thalamocortical projections. By using this framework, we present three main findings: 1) type II corticothalamic terminals (presumed drivers) from the AI and AAF are found chiefly in the MGBd, whereas type I corticothalamic terminals (presumed modulators) are found chiefly in the MGBv; 2) the MGBd receives corticothalamic projections from layer 5 of all areas of the AC and layer 6 of the nonlemniscal

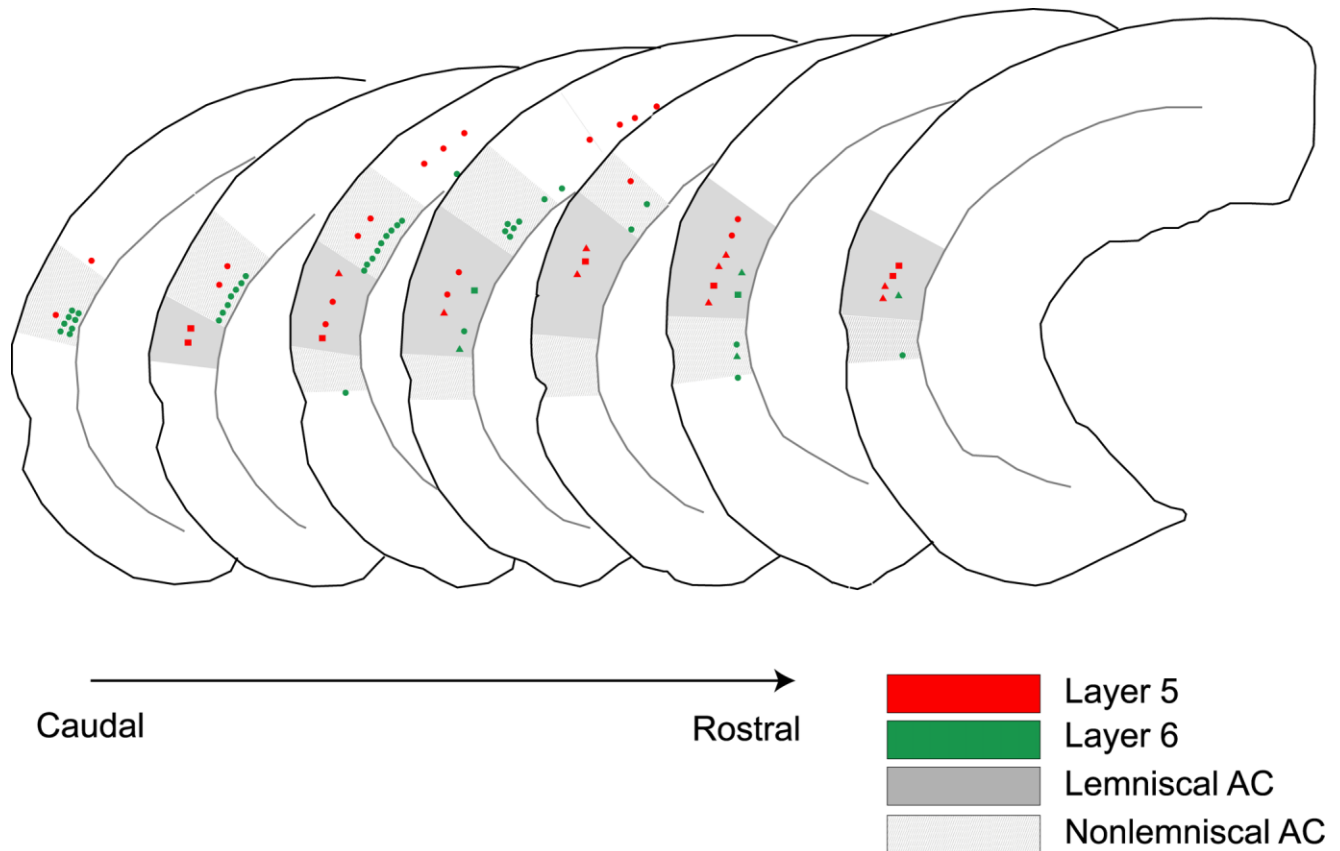


Fig. 9. Summary data from all three MGBd injections illustrating the distribution of retrogradely labeled corticothalamic neurons. Areas in gray represent the lemniscal portions of the AC (AI and AAF), and stippled areas represent the nonlemniscal areas (DP and AII). Circles, animal 10.26.06.1L; squares, animal 9.22.06.2R; triangles, animal 10.10.06.1L. For abbreviations, see list.

AC, whereas the MGBv receives layer 6 corticothalamic input only from the lemniscal AC; and 3) there is thalamocortical-corticothalamic reciprocity in the projections involving the MGBv, whereas there is no reciprocity in the MGBd-lemniscal AC pathway, with the corticothalamic component involving type II terminals from layer 5. The lack of reciprocity in the latter system raises the possibility that the MGBd may be important for relaying information between different cortical areas, which will be further explored below.

Methodological considerations

This study, like virtually all bulk labeling techniques, is subject to the problem of having our experimental findings contaminated by en passant axons taking up label. For the lemniscal AC injections, it is possible, although unlikely, that the large-terminal MGBd labeling was due to axons from the infragranular layers of the nonlemniscal AC coursing through the injection zone prior to projecting to the MGBd. We feel that this is unlikely because the corticofugal projections from the nonlemniscal AC project into the subcortical white matter immediately after leaving the AC without coursing through other cortical areas (Arnault and Roger, 1990; Budinger et al., 2000b; Cruikshank et al., 2002). In the case of the MGB injections, it has been shown in the rat that there are relatively few

fibers passing through the MGBd and MGBv proper (Clerici and Coleman, 1990). In addition, the fiber bundles that do run near the MGBd and MGBv (likely branches from the optic tract, brachium of the superior colliculus, and brachium of the inferior colliculus) tend to course ventrolaterally to dorsomedially, such that both MGBv and MGBd injections would be susceptible to axonal uptake artifact, and therefore this potential source of artifact could not explain our differential findings in terms of MGBd and MGBv injections.

A second concern is that we have concluded that the MGBd-layer 5 large-terminal system is organized in a nonreciprocal fashion with the AC based on the absence of particular findings. Specifically, this conclusion is based on the absence of retrogradely labeled cell bodies in the MGBd after lemniscal AC injection and the absence of anterograde labeling to the middle layers of the lemniscal AC after MGBd injection. However, because there are clearly significant numbers of retrogradely labeled cells in the MGBv after lemniscal AC injection, and anterograde terminals in the nonlemniscal AC after MGBd injection, the previously mentioned absence of findings cannot be attributed to a lack of sensitivity of our tracer in either the anterograde or retrograde direction.

Finally, the small numbers of corticothalamic cell bodies labeled in the current study are of some concern, particu-

larly after MGBd injections. This is likely related to the very small injections that were needed to ensure lack of spillover into the MGBv. Despite the relatively small numbers of neurons labeled, the differences in their distributions were so dramatic and statistically significant (e.g., 29/41 layer 5 corticothalamic neurons after MGBd injection, vs. 2/214 after MGBv injection, and see distribution of layer 5 and 6 neurons in Figs. 6 and 7) that larger numbers were not necessary to draw our conclusions.

Comparison with other work on corticothalamic projections

Type II corticothalamic terminals have been found in the higher order portions of the visual and somatosensory thalamus (Mathers, 1972; Hoogland et al., 1987; Rockland, 1994; Bourassa et al., 1995; Liao et al., 2006) as well as the MGBd of rat, cat, and monkey (Ojima, 1994; Bajo, 1995; Winer et al., 1999; Hazama et al., 2004). In the cat, these projections retain their topographic relationships (Takanayagi and Ojima, 2006), suggesting that there is connectional specificity compatible with a specific role in information processing. The density of type II terminals appears to be slightly smaller in our preparation than in other studies, but this is likely related to our small injection sizes. Note that, despite the relatively small numbers of type II terminals in the MGBd, they can have disproportionately large impact on their thalamic targets. For example, in the lateral geniculate nucleus (LGN) of the cat, which is the only system for which there are substantial quantitative data, synapses from equivalent type II terminals (from the retina) account for only 7% of all synapses (Van Horn et al., 2000). Furthermore, these terminals are the only ones making multiple synapses (roughly nine each; Van Horn et al., 2000), so the estimate of type II terminals, regardless of origin, reduces to less than 2% of the total. In addition, type II terminals are less frequent in higher order than first order relays (Huppe-Georges et al., 2006; Van Horn and Sherman, 2007). Thus, in higher order relays like the MGBd, our observation of scarce type II terminals is consistent with other observations.

The resemblance of large corticothalamic terminals to ascending projections innervating the primary thalamic sensory nuclei suggests that they carry information in a feedforward manner as part of a cortico-thalamo-cortical circuit (Guillery, 1995; Sherman and Guillery, 2006). This is supported by physiological findings in the somatosensory and visual systems, in which two types of corticothalamic terminal EPSPs were found in the posterior-medial nucleus (POm; a higher order somatosensory relay) and the lateral posterior nucleus (LP; a higher order visual relay): large, all-or-none EPSPs showing paired-pulse depression and no activation of metabotropic glutamate receptors (drivers, resembling retinogeniculate synapses), and small, graded EPSPs with paired-pulse facilitation and a clear participation of metabotropic glutamate receptors (modulators; Li et al., 2003; Reichova and Sherman 2004). Further, Reichova and Sherman (2004) showed that the driver-type profile was only found after stimulating in layer 5 of the barrel cortex. (The cortex was not retained in the Li et al. study.) This suggests, as is further explored below, that the driver terminals emanate from layer 5.

In the auditory system, corticothalamic drivers would imply that many or all MGBd neurons derive their acoustic response properties via this cortical projection. The reports that MGBd neurons respond to sound with long latency and have broad tuning curves (similar to responses in the AC) is consistent with this hypothesis (Calford, 1983; Bordi and LeDoux, 1994a,b; Llano and Feng, 1999). Although it is possible that these response properties can be transmitted via the external and dorsal cortices of the IC (Calford and Aitkin, 1983; LeDoux et al., 1985), it has not been established that these areas provide driving input to the MGBd. Ultrastructural analysis of the IC to MGBd pathway showed that the afferent terminals are smaller, and synapse on smaller dendrites, than the terminals of the IC to MGBv pathway (Bartlett et al., 2000). Physiological studies of the IC to MGBd pathway (Hu et al., 1994; Bartlett and Smith, 1999, 2002) have been compromised by the electrical stimulation of cut axons in the brachium of the IC, leaving open the possibility that branched corticotectal fibers (which send large terminal branches to the higher order somatosensory and visual thalamus; Bourassa and Deschenes, 1995; Bourassa et al., 1995) were stimulated.

Even so, Bartlett and Smith (2002) found a trend for MGBd neurons to show greater paired-pulse facilitation; they also found that a higher relative proportion of stellate cells (only found in the MGBd) show long-term depolarization to tetanic stimulation, which is suggestive of activation of metabotropic glutamate receptors (both hallmarks of modulator input; Sherman and Guillery, 1998, 2006). Although the proposition that the AC, rather than the shell nuclei of the IC, drives MGBd neurons has yet to be fully explored, it is possible that the MGBd may in fact have a mixture of first and higher order circuits within it, with individual neurons receiving input from the tectum or cortex, respectively, similar to the heterogeneous organization of the pulvinar, which has both tecto-recipient and striate-recipient zones (Updyke, 1977; Berson and Graybiel, 1978; Mason and Groos, 1981).

Type II terminals were also occasionally found in the MGBm and the PP, which are part of the "paralamina" (Herkenham, 1980) or "associated sensory" nuclei (Winer and Morest, 1983). Large corticothalamic terminals have also been found in the MGBm in the cat (Ojima, 1994; Winer et al., 1999), although, similar to our study, these were greatly outnumbered by those in the MGBd. In addition, large corticothalamic terminals have been seen in the ventral shell area of the somatosensory thalamus after somatosensory cortex injection (Liao et al., 2006). The functional significance of these paralamina terminals is not clear. However, like the MGBd, MGBm neurons tend to show longer response latencies and broader frequency tuning than in the MGBv (Calford, 1983; Bordi and LeDoux, 1994a; Llano and Feng, 1999), so it is possible that higher order circuits exist in the MGBm and play a similar role to that postulated for the MGBd.

Alternatively, given the widespread AC projections of paralamina neurons, drivers to this group could increase excitability across large areas of AC (Metherate and Cruikshank, 1999; Linke and Schwegler, 2000; Sukov and Barth, 2001; Smith et al., 2006) or could transmit information to their other known targets, such as the basal ganglia, amygdala, or inferior colliculus (LeDoux et al., 1985; Winer et al., 2002). Alternatively, because in many respects the paralamina group resembles the intralaminar

nar nuclei, having a decreased expression of low-threshold Ca-spiking, and sending projections to the basal ganglia as well as layer 1 across the temporal cortex (Linke and Schwegler, 2000; Smith et al., 2006), drivers to this group could lead to activation across large expanses of the auditory cortex, possibly to increase excitability in these regions (Sukov and Barth, 2001), although their point-to-point connective specificity, at least in the MGBd, might argue against this (Takanayagi and Ojima, 2006). This topic awaits further investigation.

Laminar organization of corticothalamic projections

We have found that the MGBd derives its cortical input from both layer 5 and layer 6 of the AC, whereas the MGBv derives its input exclusively from layer 6. In addition, MGBd corticothalamic input is segregated such that layer 5 and 6 inputs are derived from the nonlemniscal areas of the AC (AII and DP), whereas the lemniscal areas (AI and AAF) only send layer 5 inputs. This is quite similar to the findings in the cat visual system, in which after injection of wheat germ agglutinin-horseradish peroxidase (WGA-HRP) into the striate-recipient zone of LP, layer 5 and 6 neurons were retrogradely labeled in areas 19, 20, and 21, whereas layer 5 labeled cells were only found in areas 17 and 18 (Abramson and Chalupa, 1985). Similarly, in the rat somatosensory system, layer 5 labeling was only seen after injection of fluorescent microspheres into the POM and not into the ventral posterior region (a first order somatosensory relay; Killackey and Sherman, 2003). However, unlike our data, Killackey and Sherman did find layer 6b label in the barrel cortex after POM injection. This is possibly related to the higher sensitivity of the fluorescent microspheres than 3,000 MW BDA for retrograde transport, which is evident in the large numbers of neurons labeled in their study, or possibly to interspecies or intersystem differences. The finding that the POM projects to the granular layers of the barrel field (Lu and Lin, 1993; Bureau et al., 2006), but that MGBd does not project to the granular layers of the AI or AAF (current study), suggests that layer 6 feedback may only be found in areas that receive thalamocortical input in the middle layers of the cortex.

In addition, we found that although the majority of layer 6 corticothalamic input to both the MGBd and MGBv is derived from layer 6a, a substantial minority of the projections (27%) to the MGBd emanate from layer 6b. The finding that most of the lemniscal AC-to-MGBv pathway emanates from layer 6a is consistent with findings from the rabbit (deVenecia et al., 1998), but not the cat (Prieto and Winer, 1999), in which corticothalamic neurons were evenly distributed throughout layer 6. The discrepancy between the latter study and ours may be related to the criterion used to define layer 6b, which in the current study was limited to the lower band of high cellular density within approximately 100 μm of the cortical/subcortical white matter border. Outside of the auditory system, an increased proportion of layer 6b corticothalamic neurons that project to the HO portions of the sensory thalamus have been found in the barrel cortex and the primary visual cortex (Bourassa and Deschenes, 1995; Bourassa et al., 1995; Killackey and Sherman, 2003; Usrey and Fitzpatrick, 1996).

The differences in sublaminar location also correspond with different morphologies. Zhang and Deschenes (1997),

although only working in layer 6a of barrel cortex, found that after juxtacellular injection of biocytin, HO-projecting corticothalamic neurons showed greater lateral extension of projections, often across multiple barrels. Usrey and Fitzpatrick (1996) found that layer 6b corticothalamic pyramidal cells in the tree shrew showed a greater degree of branching in the vertical dimension, often branching into layer 1. These data suggest that HO-projecting layer 6 neurons may integrate information from a greater area than FO-projecting neurons, which would be consistent with the proposed reciprocal nature of layer 6 corticothalamic projections. That is, because layer 6b projections can branch to innervate both HO and FO thalamic relays (Bourassa and Deschenes, 1995; Bourassa et al., 1995), it is expected that they would receive thalamocortical input from HO and FO regions, either directly into the same column, or via collateral projections from higher order to lower order cortical regions.

Lack of reciprocity in thalamocortical systems

Although early neurodegeneration studies were suggestive of relatively strict reciprocity between the auditory thalamus and cortex (Diamond et al., 1969), later work using more sensitive tracers produced mixed results. Winer and Larue (1987) used a combination of HRP and tritiated leucine injections into the rat AC and found areal reciprocity intermixed with small zones of nonreciprocity within all MG subdivisions. In the visual system, Van Horn and Sherman (2004) injected BDA into large areas of the cat visual cortex (areas 17, 18, 19, and 21) and found three types of zones in the visual thalamus: nonreciprocal zones in the LP-pulvinar with anterogradely labeled large without retrogradely labeled cell bodies, and two reciprocal zones: one in the LP-pulvinar, with primarily small terminals, and one in the LGN, with only small terminals. In contrast, Huppe-Georges et al., (2006) demonstrated overlap of large terminals and thalamocortical cell bodies in the lateral region of the LP (LPI) after area 17 injection of BDA but did not comment about the distribution of reciprocal vs. nonreciprocal zones in the thalamus. The observed overlap is likely related to the branching patterns of TC neurons from the LPI of the cat, which send a branch to the posteromedial lateral suprasylvian cortex (a higher order region of visual cortex) and area 17 (Tong and Spear, 1986; Miceli et al., 1991), likely to layer 1 (cat: Abramson and Chalupa, 1985; monkey: Rockland et al., 1999). Our injections tended to avoid layer 1, so this may account for this discrepancy. On the other hand, such branching patterns may not exist in mouse auditory nonlemniscal thalamocortical neurons, although there is some evidence for extensive lateral branching of lemniscal thalamocortical neurons in juvenile rabbits (de Venecia and McMullen, 1994). Finally, in the somatosensory system, after tracer cocktail injections into the parietal cortex of macaques, Darian-Smith et al. (1999) described zones of nonreciprocity in the lateral portion of the ventral posterolateral nucleus and pulvinar with corticothalamic terminations in areas without backfilled thalamocortical cells, with a greater dissociation in the pulvinar.

This convergence of evidence from multiple sensory systems, combined with the current work, suggests that nonreciprocity between the thalamus and cortex, rather than being an exception (Deschenes et al., 1998), may in fact be one of the organizing principles of higher order

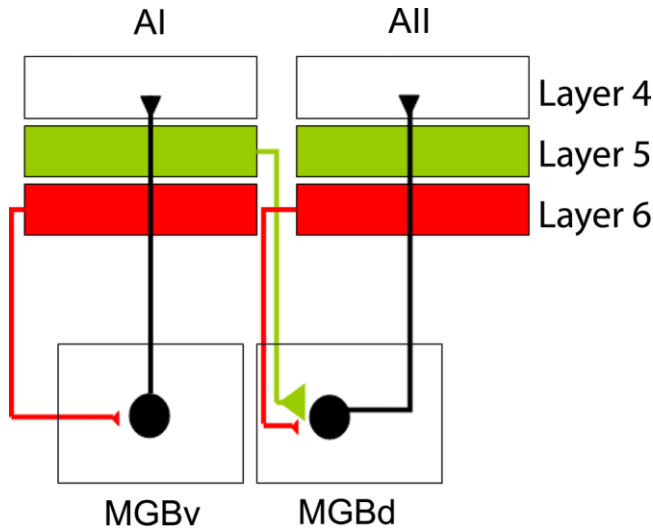


Fig. 10. Diagram illustrating our proposed cortico-thalamo-cortical model of cortical processing. In this model, information reaches the lemniscal AC via a projection from the MGBv to layer 4 of either the AAF or the AI. From here, a layer 5 pyramidal projects to the MGBd, where a thalamocortical relay cell projects to layer 4 of the nonlemniscal AC (DP or AII). From the nonlemniscal AC, a layer 6 projection is sent to the MGBd, adhering to the principle that all thalamocortical projections, whether coming from the first or higher order thalamus, receive a modulator, reciprocal projection from layer 6. For abbreviations, see list.

thalamocortical systems. Further, by the “no strong loops” hypothesis of Crick and Koch (1998), the driver properties of type II synapses (Li et al., 2003; Reichova and Sherman, 2004) would prohibit them from being included in a reciprocal thalamocortical-corticothalamic circuit, which could lead to unstable oscillations (Crick and Koch, 1998). In the context of the auditory system, we propose that the neurons in the MGBd receive layer 5 driver projections from lower order areas of the AC and then project to higher cortical areas. We propose that there are two types of auditory thalamocortical circuits: 1) a reciprocal circuit originating in the MGBv or MGBd, projecting mainly to layers 4 and 6 of the lemniscal or nonlemniscal AC, respectively, and then projecting from layer 6 to the thalamic region of origin via modulator, type I terminals; and 2) a non-reciprocal circuit, originating in layer 5 of the lemniscal AC, projecting to the MGBd via driver, type II terminals, and then projecting mainly to layers 4 and 6 of the nonlemniscal AC.

Finally, embedded in this nonreciprocal cortico-thalamo-cortical circuit is a reciprocal circuit involving a layer 6 corticothalamic projection and linking the MGBd and the nonlemniscal AC, adhering to the principle that all thalamocortical projections, whether coming from the FO or HO thalamus, receive a modulator, reciprocal projection from layer 6 (Fig. 10). The finding that a major component of nonlemniscal thalamocortical projection is directed to the middle cortical layers (Hashikawa et al., 1995; Huang and Winer, 2000; Fig. 8 of current study), and that nonlemniscal thalamocortical layer 4 synapses have a driver-type physiological signature (Lee and Sherman, 2006), supports the latter

part of this circuit. Note that our finding of retrogradely labeled layer 5 neurons in the nonlemniscal AC after MGBd injection suggests that both reciprocal and non-reciprocal circuits may be found within the MGBd. This would be consistent with work in the higher order visual thalamus, in which both reciprocal and nonreciprocal zones have been found (Van Horn and Sherman, 2004) and suggests that multiple pathways may exist through the MGBd. Further, the projection of the MGBd to multiple cortical fields suggests that the organization of the MGBd may resemble that of the pulvinar, in which a single higher order thalamic region projects to multiple cortical areas (Benevento and Rezak, 1976).

One important facet of the proposed scheme is the driving nature of the nonlemniscal thalamocortical projection. Others have proposed a modulatory role for this projection (Olshausen et al., 1993; Jones, 2002), partly based on its projection to layer 1 of the cortex. It is important to note that in the higher order regions of cortex, nonlemniscal thalamocortical neurons project to the middle cortical layers, as well as layer 1, and may in fact send collaterals to layer 1 of the primary sensory cortex. For example, in the monkey auditory system, it was shown that MGBd neurons were labeled after fast blue-soaked filter paper was placed over the exposed surface of the AI but that anterograde label directly placed into the MGBd labeled the middle cortical layers of the belt areas of the cortex (Molinari et al., 1995; Hashikawa et al., 1995). This suggests that the layer 1 projections in the AI may represent collaterals from an MGBd-to-AII projection.

Indeed, the current study and work of others (Hashikawa et al., 1995; Huang and Winer, 2000) have shown that the MGBd-nonlemniscal AC pathway is notable for projections to layers 4 and 6, as in the lemniscal pathway, as well as layer 1. Further, the current study demonstrates layer 1 projections from the MGBd to the AI (Fig. 8), also consistent with the idea that nonlemniscal thalamocortical axons send projections to the middle layers of higher order cortical fields as well as to layer 1 of lower order fields, possibly via branching of individual axons. In addition, recent work has established that thalamocortical projections from the POM and the MGBd to layer 4 of the SII and AII, respectively, share the characteristics of driver inputs (large EPSPs, paired-pulse depression, lack of metabotropic glutamate receptor responses) seen in lemniscal layer 4 TC synapses (Lee and Sherman, 2006). These studies, as well as the current work, suggest that projections from the HO thalamus to the nonlemniscal cortex have targets in the middle cortical layers, have driver-type physiology, and may be responsible, at least in part, for the receptive field properties of higher order cortical neurons.

ACKNOWLEDGMENTS

We thankfully acknowledge the technical assistance of Susan VanHorn of the Department of Neurobiology and the Central Microscopy Imaging Center at the State University of New York, Stony Brook.

LITERATURE CITED

Abramson BP, Chalupa LM. 1985. The laminar distribution of cortical connections with the tecto and cortico-recipient zones in the cat's lateral posterior nucleus. *Neuroscience* 15:81–95.

- Arnault P, Roger M. 1990. Ventral temporal cortex in the rat: connections of secondary auditory areas Te2 and Te3. *J Comp Neurol* 302:110–123.
- Bajo VM, Rouiller EM, Welker E, Clarke S, Villa AE, de Ribaupierre Y, de Ribaupierre F. 1995. Morphology and spatial distribution of corticothalamic terminals originating from the cat auditory cortex. *Hear Res* 83:161–174.
- Bartlett EL, Smith PH. 1999. Anatomic, intrinsic, and synaptic properties of dorsal and ventral division neurons in rat medial geniculate body. *J Neurophysiol* 81:1999–2016.
- Bartlett EL, Smith PH. 2002. Effects of paired-pulse and repetitive stimulation on neurons in the rat medial geniculate body. *Neuroscience* 113:957–974.
- Bartlett EL, Stark JM, Guillery RW, Smith PH. 2000. Comparison of the fine structure of cortical and collicular terminals in the rat medial geniculate body. *Neuroscience* 100:811–828.
- Benevento LA, Rezak M. 1976. The cortical projections of the inferior pulvinar and adjacent lateral pulvinar in the rhesus monkey (*Macaca mulatta*): an autoradiographic study. *Brain Res* 127:1–24.
- Berson DM, Graybiel AM. 1978. Parallel thalamic zones in the LP-pulvinar complex of the cat identified by their afferent and efferent connections. *Brain Res* 147:139–148.
- Berson DM, Graybiel AM. 1983. Organization of the striate-recipient zone of the cat's lateralis posterior-pulvinar complex and its relations with the geniculostriate system. *Neuroscience* 9:337–372.
- Bordi F, LeDoux JE. 1994a. Response properties of single units in areas of rat auditory thalamus that project to the amygdala. I. Acoustic discharge patterns and frequency receptive fields. *Exp Brain Res* 98:261–274.
- Bordi F, LeDoux JE. 1994b. Response properties of single units in areas of rat auditory thalamus that project to the amygdala. II. Cells receiving convergent auditory and somatosensory inputs and cells antidromically activated by amygdala stimulation. *Exp Brain Res* 98:275–286.
- Bourassa J, Deschenes M. 1995. Corticothalamic projections from the primary visual cortex in rats: a single fiber study using biocytin as an anterograde tracer. *Neuroscience* 66:253–263.
- Bourassa J, Pinault D, Deschenes M. 1995. Corticothalamic projections from the cortical barrel field to the somatosensory thalamus in rats: a single-fibre study using biocytin as an anterograde tracer. *Eur J Neurosci* 7:19–30.
- Budinger E, Heil P, Scheich H. 2000a. Functional organization of auditory cortex in the Mongolian gerbil (*Meriones unguiculatus*). III. Anatomical subdivisions and corticocortical connections. *Eur J Neurosci* 12:2425–2451.
- Budinger E, Heil P, Scheich H. 2000b. Functional organization of auditory cortex in the Mongolian gerbil (*Meriones unguiculatus*). IV. Connections with anatomically characterized subcortical structures. *Eur J Neurosci* 12:2452–2474.
- Bureau I, von Saint Paul F, Svoboda K. 2006. Interdigitated paralemnisal and lemniscal pathways in the mouse barrel cortex. *PLoS Biol* 4:e382.
- Calford MB. 1983. The parcellation of the medial geniculate body of the cat defined by the auditory response properties of single units. *J Neurosci* 3:2350–2364.
- Calford MB, Aitkin LM. 1983. Ascending projections to the medial geniculate body of the cat: evidence for multiple, parallel auditory pathways through thalamus. *J Neurosci* 3:2365–2380.
- Caviness VS Jr. 1975. Architectonic map of neocortex of the normal mouse. *J Comp Neurol* 164:247–263.
- Clerici WJ, Coleman JR. 1990. Anatomy of the rat medial geniculate body: I. Cytoarchitecture, myeloarchitecture, and neocortical connectivity. *J Comp Neurol* 297:14–31.
- Crick F, Koch C. 1998. Constraints on cortical and thalamic projections: the no-strong-loops hypothesis. *Nature* 391:245–250.
- Cruikshank S J, Killackey HP, Metherate R. 2001. Parvalbumin and calbindin are differentially distributed within primary and secondary subregions of the mouse auditory forebrain. *Neuroscience* 105:553–569.
- Cruikshank S J, Rose HJ, Metherate R. 2002. Auditory thalamocortical synaptic transmission in vitro. *J Neurophysiol* 87:361–384.
- Darian-Smith C, Tan A, Edwards S. 1999. Comparing thalamocortical and corticothalamic microstructure and spatial reciprocity in the macaque ventral posterolateral nucleus (VPLc) and medial pulvinar. *J Comp Neurol* 410:211–234.
- Deschenes M, Veinante P, Zhang ZW. 1998. The organization of corticothalamic projections: reciprocity versus parity. *Brain Res Brain Res Rev* 28:286–308.
- de Venecia RK McMullen NT. 1994. Single thalamocortical axons diverge to multiple patches in neonatal auditory cortex. *Brain Res Dev Brain Res* 81:135–142.
- de Venecia RK, Smelser CB, Lossman SD, McMullen NT. 1995. Complementary expression of parvalbumin and calbindin D-28k delineates subdivisions of the rabbit medial geniculate body. *J Comp Neurol* 359:595–612.
- de Venecia RK, Smelser CB, McMullen NT. 1998. Parvalbumin is expressed in a reciprocal circuit linking the medial geniculate body and auditory neocortex in the rabbit. *J Comp Neurol* 400:349–362.
- Diamond IT, Jones EG, Powell TPS. 1969. The projection of the auditory cortex upon the diencephalon and brainstem in the cat. *Brain Res* 15:305–340.
- Donishi T, Kimura A, Okamoto K, Tamai Y. 2006. "Ventral" area in the rat auditory cortex: a major auditory field connected with the dorsal division of the medial geniculate body. *Neuroscience* 141:1553–1567.
- Gonzalez-Lima F, Cada A. 1994. Cytochrome oxidase activity in the auditory system of the mouse: a qualitative and quantitative histochemical study. *Neuroscience* 63:559–578.
- Guillery RW. 1966. A study of Golgi preparations from the dorsal lateral geniculate nucleus of the adult cat. *J Comp Neurol* 128:21–50.
- Guillery RW. 1995. Anatomical evidence concerning the role of the thalamus in corticocortical communication: a brief review. *J Anat* 187:83–592.
- Hashikawa T, Rausell E, Molinari M, Jones EG. 1991. Parvalbumin- and calbindin-containing neurons in the monkey medial geniculate complex: differential distribution and cortical layer specific projections. *Brain Res* 544:335–341.
- Hashikawa T, Molinari M, Rausell E, Jones EG. 1995. Patchy and laminar terminations of medial geniculate axons in monkey auditory cortex. *J Comp Neurol* 362:195–208.
- Hazama M., Kimura A, Donishi T, Sakoda T, Tamai Y. 2004. Topography of corticothalamic projections from the auditory cortex of the rat. *Neuroscience* 124:655–667.
- Herkenham M. 1980. Laminar organization of thalamic projections to the rat neocortex. *Science* 207:532–535.
- Hofstetter KM, Ehret G. 1992. The auditory cortex of the mouse: connections of the ultrasonic field. *J Comp Neurol* 323:370–386.
- Hoogland PV, Welker E, Loos H. 1987. Organization of the projections from barrel cortex to thalamus in mice studied with *Phaseolus vulgaris*-leucoagglutinin and HRP. *Exp Brain Res* 68:73–87.
- Hu B, Senatorov V, Mooney D. 1994. Lemniscal and non-lemniscal synaptic transmission in rat auditory thalamus. *J Physiol* 479:217–231.
- Huang CL, Winer JA. 2000. Auditory thalamocortical projections in the cat: laminar and areal patterns of input. *J Comp Neurol* 427:302–331.
- Huppe-Georges F, Bickford ME, Boire D, Ptitto M., Casanova C. 2006. Distribution, morphology, and synaptic targets of corticothalamic terminals in the cat lateral posterior-pulvinar complex that originate from the posteromedial lateral suprasylvian cortex. *J Comp Neurol* 497:847–863.
- Jones EG. 2002. Thalamic circuitry and thalamocortical synchrony. *Philos Trans R Soc Lond B Biol Sci* 357:1659–1673.
- Killackey HP, Sherman SM. 2003. Corticothalamic projections from the rat primary somatosensory cortex. *J Neurosci* 23:7381–7384.
- Kimura A, Donishi T, Sakoda T, Hazama M., Tamai, Y. 2003. Auditory thalamic nuclei projections to temporal cortex in rat. *Neuroscience* 117:1003–1016.
- Krubitzer LA, Kaas JH. 1987. Thalamic connections of three representations of the body surface in somatosensory cortex of gray squirrels. *J Comp Neurol* 265:549–580.
- LeDoux JE, Ruggiero DA, Reis DJ. 1985. Projections to the subcortical forebrain from anatomically defined regions of the medial geniculate body in the rat. *J Comp Neurol* 242:182–213.
- Lee CC, Sherman SM. 2006. The thalamocortical synapse: driver properties from higher order nuclei. *Soc Neurosci Abstract* #446.4.
- Li J, Guido W, Bickford ME. 2003. Two distinct types of corticothalamic EPSPs and their contribution to short-term synaptic plasticity. *J Neurophysiol* 90:3429–3440.

- Liao C, Yen C, Simpson K, Lin RC. 2006. Prevalence of giant terminal inputs in rat: from primary and secondary somatosensory cortex to dorsal thalamus. *Soc Neurosci Abstract* #446.6.
- Linke R, Schwegler H. 2000. Convergent and complementary projections of the caudal paralaminar thalamic nuclei to rat temporal and insular cortex. *Cereb Cortex* 10:753–771.
- Llano DA, Feng AS. 1999. Response characteristics of neurons in the medial geniculate body of the little brown bat to simple and temporally-patterned sounds. *J Comp Physiol [A]* 184:371–385.
- Lu SM, Lin RCS. 1993. Thalamic afferents of the rat barrel cortex: a light- and electronmicroscopic study using *Phaseolus vulgaris* leucoagglutinin as an anterograde tracer. *Somatosens Mot Res* 10:1–16.
- Mason R, Groos GA. 1981. Cortico-recipient and tecto-recipient visual zones in the rat's lateral posterior (pulvinar) nucleus: an anatomical study. *Neurosci Lett* 25:107–112.
- Mathers LH. 1972. The synaptic organization of the cortical projection to the pulvinar of the squirrel monkey. *J Comp Neurol* 146:43–60.
- Merzenich MM, Knight PL, Roth GL. 1975. Representation of cochlea within primary auditory cortex in the cat. *J Neurophysiol* 38:231–249.
- Metherate R, Cruikshank SJ. 1999. Thalamocortical inputs trigger a propagating envelope of gamma-band activity in auditory cortex in vitro. *Exp Brain Res* 126:160–174.
- Miceli D, Reperant J, Marchand L, Ward R, Vesselkin N. 1991. Divergence and collateral axon branching in subsystems of visual cortical projections from the cat lateral posterior nucleus. *J Hirnforsch* 32:165–173.
- Molinari M, Dell'Anna ME, Rausell E, Leggio MG, Hashikawa T, Jones EG. 1995. Auditory thalamocortical pathways defined in monkeys by calcium-binding protein immunoreactivity. *J Comp Neurol* 362:171–194.
- Morel A, Rouiller E, de Ribaupierre Y, de Ribaupierre F. 1987. Tonotopic organization in the medial geniculate body (MGB) of lightly anesthetized cats. *Exp Brain Res* 69:24–42.
- Morest DK. 1965. The laminar structure of the medial geniculate body of the cat. *J Anat* 99:143–160.
- Nelson RJ, Kaas JH. 1981. Connections of the ventroposterior nucleus of the thalamus with the body surface representations in cortical areas 3b and 1 of the cynomolgus macaque (*Macaca fascicularis*). *J Comp Neurol* 199:29–64.
- Ojima H. 1994. Terminal morphology and distribution of corticothalamic fibers originating from layers 5 and 6 of cat primary auditory cortex. *Cereb Cortex* 4:646–663.
- Olshausen B, Anderson, Van Essen DC. 1993. A neurobiological model of visual attention and invariant pattern recognition based on dynamic routing of information. *J Neurosci* 13:4700–4719.
- Paxinos G, Franklin KBJ. 2001. *The mouse brain in stereotaxic coordinates*. San Diego: Academic Press.
- Pontes C, Reis FF, Sousa-Pinto A. 1975. The auditory cortical projections onto the medial geniculate body in the cat. An experimental anatomical study with silver and autoradiographic methods. *Brain Res* 91:43–63.
- Prieto JJ, Winer JA. 1999. Layer VI in cat primary auditory cortex: Golgi study and sublaminal origins of projection neurons. *J Comp Neurol* 404:332–358.
- Radies H, Brandner S. 1991. Functional organization of the auditory thalamus in the guinea pig. *Exp Brain Res* 86:384–392.
- Reichova I, Sherman SM. 2004. Somatosensory corticothalamic projections: distinguishing drivers from modulators. *J Neurophysiol* 92:2185–2197.
- Robertson RT. 1977. Bidirectional movement of horseradish peroxidase and the demonstration of reciprocal thalamocortical connections. *Brain Res* 130:538–544.
- Rockland KS. 1994. Further evidence for two types of corticopulvinar neurons. *Neuroreport* 5:1865–1868.
- Rockland KS, Andresen J, Cowie RJ, Robinson DL. 1999. Single axon analysis of pulvinocortical connections to several visual areas in the macaque. *J Comp Neurol* 406:221–250.
- Roger M, Arnault P. 1989. Anatomical study of the connections of the primary auditory area in the rat. *J Comp Neurol* 287:339–356.
- Rouiller EM, Welker E. 1991. Morphology of corticothalamic terminals arising from the auditory cortex of the rat: a *Phaseolus vulgaris*-leucoagglutinin (PHA-L) tracing study. *Hear Res* 56:179–190.
- Rouiller EM, Simm GM, Villa AE, de Ribaupierre Y, de Ribaupierre F. 1991. Auditory corticocortical interconnections in the cat: evidence for parallel and hierarchical arrangement of the auditory cortical areas. *Exp Brain Res* 86:483–505.
- Sally SL, Kelly JB. 1988. Organization of auditory cortex in the albino rat: sound frequency. *J Neurophysiol* 59:1627–1638.
- Sherman SM, Guillery RW. 1998. On the actions that one nerve cell can have on another: distinguishing “drivers” from “modulators.” *Proc Natl Acad Sci U S A* 95:7121–7126.
- Sherman SM, Guillery RW. 2002. The role of the thalamus in the flow of information to the cortex. *Philos Trans R Soc Lond B Biol Sci* 357:1695–1708.
- Sherman SM, Guillery RW. 2006. *Exploring the thalamus and its role in cortical function*. Cambridge, MA: MIT Press.
- Shi CJ, Cassell MD. 1997. Cortical, thalamic, and amygdaloid projections of rat temporal cortex. *J Comp Neurol* 382:153–175.
- Slaytor E. 1970. *Optical methods in biology*. New York: Wiley-Interscience.
- Smith PH, Bartlett EL, Kowalkowski A. 2006. Unique combination of anatomy and physiology in cells of the rat paralaminar thalamic nuclei adjacent to the medial geniculate body. *J Comp Neurol* 496:314–334.
- Stiebler I. 1987. A distinct ultrasound-processing area in the auditory cortex of the mouse. *Naturwissenschaften* 74:96–97.
- Stiebler I, Neulist R, Fichtel I, Ehret G. 1997. The auditory cortex of the house mouse: left-right differences, tonotopic organization and quantitative analysis of frequency representation. *J Comp Physiol [A]* 181:559–571.
- Sukov W, Barth DS. 2001. Cellular mechanisms of thalamically evoked gamma oscillations in auditory cortex. *J Neurophysiol* 85:1235–1245.
- Takanayagi M, Ojima H. 2006. Microtopography of the dual corticothalamic projections originating from domains along the frequency axis of the cat primary auditory cortex. *Neuroscience* 142:769–780.
- Thomas H, Tillein J. 1997. Functional organization of the auditory cortex in a native Chilean rodent (*Octodon degus*). *Biol Res* 30:137–148.
- Thomas H, Tillein J, Heil P, Scheich H. 1993. Functional organization of auditory cortex in the mongolian gerbil (*Meriones unguiculatus*). I. Electrophysiological mapping of frequency representation and distinction of fields. *Eur J Neurosci* 5:882–897.
- Tong L, Spear PD. 1986. Single thalamic neurons project to both lateral suprasylvian visual cortex and area 17: a retrograde fluorescent double-labeling study. *J Comp Neurol* 246:254–264.
- Updyke BV. 1977. Topographic organization of the projections from cortical areas 17, 18 and 19 onto the thalamus, pretectum and superior colliculus in the cat. *J Comp Neurol* 173:81–122.
- Usrey WM, Fitzpatrick D. 1996. Specificity in the axonal connections of layer VI neurons in tree shrew striate cortex: evidence for distinct granular and supragranular systems. *J Neurosci* 16:1203–1218.
- Van Horn SC, Sherman SM. 2004. Differences in projection patterns between large and small corticothalamic terminals. *J Comp Neurol* 475:406–415.
- Van Horn SC, Sherman SM. 2007. Fewer driver synapses in higher order than first order thalamic relays. *Neuroscience* 146:463–470.
- Van Horn SC, Erisir A, Sherman SM. 2000. Relative distribution of synapses in the A-laminae of the lateral geniculate nucleus of the cat. *J Comp Neurol* 416:509–520.
- Vaudano E, Legg CR, Glickstein M. 1991. Afferent and efferent connections of temporal association cortex in the rat: a horseradish peroxidase study. *Eur J Neurosci* 3:317–330.
- Wallace MN, Kitzes LM, Jones EG. 1991. Chemoarchitectonic organization of the cat primary auditory cortex. *Exp Brain Res* 86:518–526.
- Winer JA, Larue DT. 1987. Patterns of reciprocity in auditory thalamocortical and corticothalamic connections: study with horseradish peroxidase and autoradiographic methods in the rat medial geniculate body. *J Comp Neurol* 257:282–315.
- Winer JA, Morest DK. 1983. The medial division of the medial geniculate body of the cat: implications for thalamic organization. *J Neurosci* 3:2629–2651.

- Winer JA, Larue DT, Huang CL. 1999. Two systems of giant axon terminals in the cat medial geniculate body: convergence of cortical and GABAergic inputs. *J Comp Neurol* 413:181–197.
- Winer JA, Chernock ML, Larue DT, Cheung SW. 2002. Descending projections to the inferior colliculus from the posterior thalamus and the auditory cortex in rat, cat, and monkey. *Hear Res* 168:181–195.
- Wong-Riley M. 1979. Changes in the visual system of monocularly sutured or enucleated cats demonstrable with cytochrome oxidase histochemistry. *Brain Res* 171:11–28.
- Wree A, Zilles K, Schleicher A. 1983. A quantitative approach to cytoarchitectonics. VIII. The areal pattern of the cortex of the albino mouse. *Anat Embryol (Berl)* 166:333–353.
- Zhang ZW, Deschenes M. 1997. Intracortical axonal projections of lamina VI cells of the primary somatosensory cortex in the rat: a single-cell labeling study. *J Neurosci* 17:6365–6379.